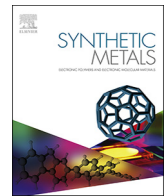




ELSEVIER

Contents lists available at ScienceDirect

Synthetic Metals

journal homepage: www.elsevier.com/locate/synmet

Isotropic metallic transport in conducting polymers

Philipp Stadler^{a,b,*}^a Linz Institute of Organic Solar Cells and Institute of Physical Chemistry, Johannes Kepler University Linz, Altenberger Straße 69, 4040 Linz, Austria^b Linz Institute of Technology, Johannes Kepler University Linz, Altenberger Straße 69, 4040 Linz, Austria

ARTICLE INFO

Keywords:

Conducting polymers
Metal-insulator transition
Isotropic metallic transport
Hall-effect
Positive magnetoconductivity
Scattering length

ABSTRACT

Conducting polymers represent an emerging class of conductors combining notable optoelectronic and thermoelectric properties; however, the electrical performance remains a limiting factor. This review provides an overview of the relevant parameters driving the rarely observed metal-insulator transition. Recent magneto-transport measurements provide clearer insight to study the proximity to the metallic state, *i.e.* the exact quantification of scattering and mobility. From that, one conclusion is the desired isotropic metallic phases depend on coherence and intermolecular radii.

1. Introduction

Conducting polymers (CPs) have emerged to a valuable class of alternative molecular conductors [1–3]. They combine excellent processability and significant conductivity appreciated in various fields of organic electronics, *e.g.* for thermoelectric active layers [4–9] and for transparent electrodes [10–15]. Since their discovery by Heeger, MacDiarmid and Shirakawa [16,17], the conductivity has shown an enormous improvement from early nematic to today (thin-film) *isotropic* systems with conductivities beyond 4000 Scm^{-1} [18–23].

In this article, we mainly treat on recent developments of the metallicity in doped poly(3,4-ethylenedioxythiophenes) (PEDOTs). One continuous goal has been the improvement of the electrical conductivity towards isotropic, metal-like and facile-processed systems. However, transport in conducting polymers is complex and depends on multiple factors such as the arrangement of the conjugated doped polycations and their corresponding anions [24,25]. The multiple interactions (covalent, ionic and weaker intermolecular bonds) can easily result in disorder such as amorphism and inhomogeneity; impurities and structural and molecular defects [26].

Fortunately, several works demonstrated that the latter extrinsic disorder can be overcome with the consequence of a metal-insulator transition (MIT, Fig. 1) [18,19,34–39,23,27–33]. For such a *metallic* conducting polymer, the transport still splits up in three regimes: Insulating or exponential regime, an intermediate transition or critical

regime and, ultimately, a metallic regime. In the insulating and transition regime, the temperature coefficient of resistivity (TCR) remains negative, as for semiconductors and disordered matter, and follows the theory of weak localization. The resistivity ρ (inverse conductivity σ) increases with temperature following a power law with an exponent β close to 0.25 (Fig. 1b and Eq. 1) [40].

$$\rho(T) \approx T^{-\beta} \quad (1)$$

At lower temperatures, in the transition regime, the power law is no longer valid. Here, the conductivity gradually decreases until reaching a minimum (σ_{\min}) at the metal-insulator transition (MIT). At temperatures below the conductivity minimum, the TCR finally turns positive and σ increases like for a crystalline metal (metallic regime).

This review discusses the parameters inducing the metal transition and the signatures of metallic transport in conducting polymers, including a discussion of the reasons for the frequent observation of extended transition regimes without explicit metal-insulator transition. The study conveys further the differences of conducting polymers compared to classic metals and elucidates the relevant factors, why present system show the metallic phase only at low temperatures and, further, what efforts are required to increase the transition temperature and, thus, the metallic nature of the polymers.

Abbreviations: CP, conducting polymer or conductive polymer; MIT, metal-insulator transition; TCR, temperature coefficient of resistivity; IRAV, infrared activated vibrations; PA, polyacetylene; PPy, polypyrrole; PANi, polyaniline; PEDOT, poly(3,4-ethylenedioxythiophene); 1D, one-dimensional; VPP, vapor-processed polymer; MFP, mean-free-path; MT, magnetotransport; ML, magnetolocalization; MC, magnetoconductivity

* Corresponding author at: Linz Institute of Organic Solar Cells and Institute of Physical Chemistry, Johannes Kepler University Linz, Altenberger Straße 69, 4040 Linz, Austria.

E-mail address: Philipp.Stadler@jku.at.

<https://doi.org/10.1016/j.synthmet.2019.06.004>

Received 19 February 2019; Received in revised form 30 May 2019; Accepted 4 June 2019

Available online 17 June 2019

0379-6779/© 2019 The Author. Published by Elsevier B.V. This is an open access article under the CC BY license

(<http://creativecommons.org/licenses/by/4.0/>).

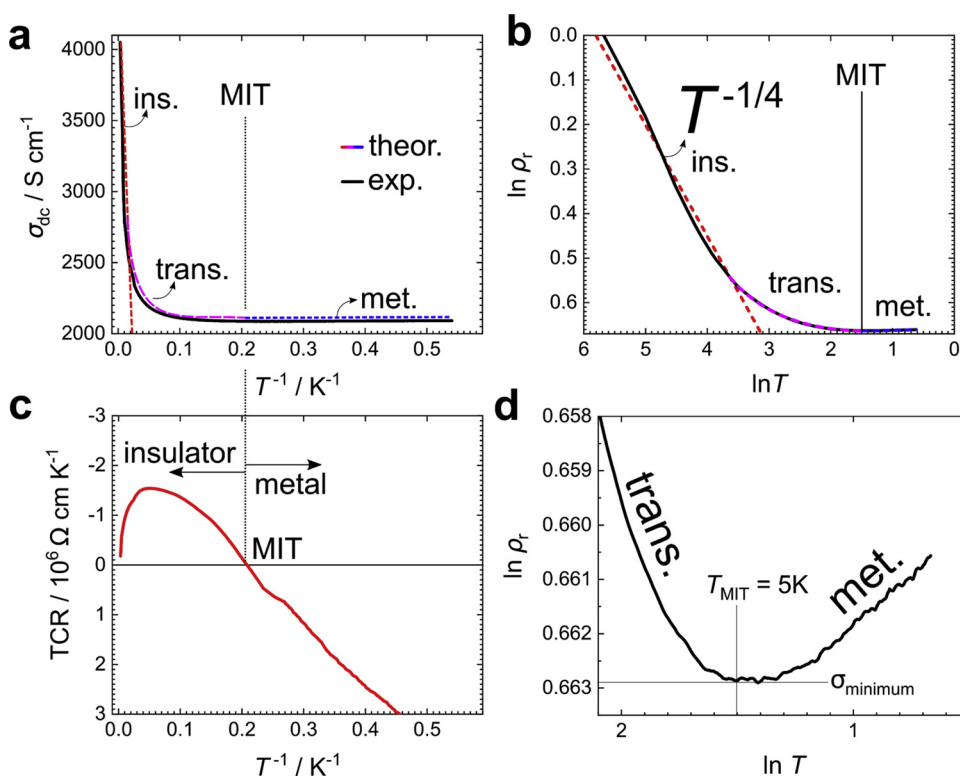


Fig. 1. Temperature profile of conductivity (σ) of an almost ideal (*i.e.* no extrinsic disorder) conducting polymer: (a) Inverse temperature plot shows the different regimes (ins. = insulator; trans. = transition; met. = metal regime). Particularly the low- T part is at first glance T -independent. (b) The logarithmic plot of the relative resistivity ($\rho_r = \rho_{300K}/\rho_T$) indicates the exponent (idealized case is $-1/4$, indicated as red dashed line) between room temperature and low temperature, the transition regime deviating from the power law and the metallic regime with the rise of conductivity (σ). (c) The temperature coefficient of resistivity (TCR) changes at the metal-insulator transition observed in the inverse temperature plot and (d) in the logarithmic plot with the local conductivity minimum at the MIT (5 K) and subsequent rise of σ as T is further decreased. Reproduced with permission from Ref. [19] (For interpretation of the references to colour in this figure legend, the reader is referred to the web version of this article).

2. Carrier localization: intrinsic and extrinsic disorder

Carrier localization in CPs is partly an intrinsic phenomenon. It originates from the phononic disorder, *i.e.* the thermal distortion caused by one-dimensionality, and the weak intermolecular bonds such as van der Waals [41]. On top, there exist extrinsic sources of disorder in general relating to defects caused by amorphism, substrate/surface effects and inhomogeneity summarized as topological, spatial and energetic disorder [19,23,27,28,42–45].

Conducting polymer research has notoriously focused the systematic exclusion of all sources of extrinsic disorder in order to break localization and achieve metallic conductivity [44,46–48]. Judiciously-processed examples have demonstrated a metallic transition at low temperatures: polypyrrole (PPy), polyacetylene (PA), and recently, poly(3,4-ethylenedioxythiophene) (PEDOT) show a low-temperature (low- T) metal-insulator transition [18,19,23,27,28]. There exists a single exceptional case of a high temperature metallic state in polyaniline (PAni), which we assign to the particular different nature of doping [49].

The discrepancy between crystalline metals and metallic CPs is the negative temperature coefficient of resistivity (TCR) observed at room temperatures. The metallic state occurs only at low- T (all around 4–7 K) in a regime, where phononic distortions become negligible.

In today's commonly used CPs, the classic metal-insulator transition is rarely observed. The residual extrinsic disorder in such films eliminates the metal-insulator transition or, shifts the transition to lower temperatures. (Fig. 1).

These commonly observed effects are well-known and, in various cases, regarded as substrate- or surface-related. Backscattering, surface inhomogeneity and defects are practically hard to avoid and require thorough processing techniques combined with subsequent post-treatment to diminish disorder. Interestingly, also the magnitude of conductivity σ at room temperatures does not exclude extrinsic disorder, as the σ is a volumetric parameter. In this context, recent works have proposed a correction term for the conductivity in molecular systems [42].

Magnetotransport (MT) represents the appropriate technique, to explore residual disorder in those polymers close to the metallic transition. MT can quantify extrinsic disorder and, on top, provide qualitative information about the origins. MT includes the measurement of the Hall-coefficient, subsequently an estimate of the band mobility, as well as the mean-free-path of scattering λ_{mfp} . These parameters represent valuable information about extrinsic disorder, the coherence among the molecules and an estimate of the intrinsic conductivity.

2.1. Intrinsic phononic disorder

Phononic disorder in conjugated polymer matter is stronger as compared to metals [50]. It represents the product of strong electron-phonon coupling emerging from molecular anisotropy (1D-character of polymers) and its impact on the weak intermolecular bonds [42]. Phononic disorder is intrinsic in doped polymers. One consistent indication is the intense infrared activated vibrations (IRAVs) [46,51]. They originate from numerous doping-activated vibronic oscillators and occur in the mid-infrared below 1500 cm^{-1} (186 meV) [52,53]. Thus, IRAVs are a first estimate of the magnitude of the coupling, since they contribute to the total phononic distortions affecting the intermolecular bonding strength.

Intermolecular transfer integrals are relevant for the metal-insulator transition; theoretically, the transition energy $k_B T_{\text{MIT}}$ is proportional to the actual bonding strength, apart from the size of the monomer, the doping and, importantly, phononic distortions [26,54,55]. Here, phonons entail characteristic merits of CPs such as the broad window of transparency [18,52,53], and active thermoelectricity [45,56] (Fig. 2).

Phononic localization is strong at room temperature; therefore, CPs possess non-metallic electrical transport at room temperature, which gradually approaches the metallic phase as temperature is decreased [33,44]. One goal in transport studies focusses the separation of intrinsic and extrinsic disorder, or, the separation of delocalized and localized carriers. Such splitting is simplified at low temperatures. Here, the conductivity profile reveals the real quality of the conducting polymer system, in particular its proximity to the isotropic metallic

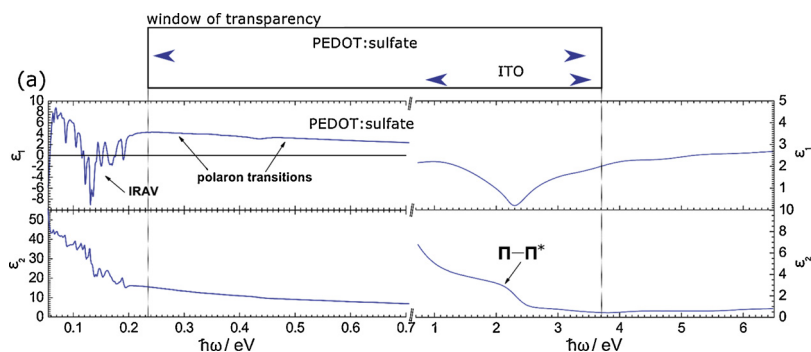


Fig. 2. Phononic distortions in CPs: Below 200 meV strong infrared-activated vibrations emerge in the mid-infrared spectrum (dielectric function) of highly-doped CPs. Reproduced with permission from Ref. [18].

state.

2.2. Extrinsic disorder

Extrinsic sources of disorder, often connoted as topological, spatial and energetic disorder, are caused by imperfection in the structure. They convey all disorder effects, which are suppressible by optimization *e.g.* by advancing the order among the chains or by implementing techniques to reduce impurities. Topological or spatial disorder relate to amorphism and inhomogeneity *e.g.* abrupt interfaces from film-processing, surface and substrate effects, solvent intercalations and presence of impurities. Energetic disorder relates more to defects in the conjugated π -system. These emerge by too harsh conditions during synthesis [57,58].

The quality of commonplace conducting polymers has increased over the years, so that today commercial products with overall low defect density are state-of-the-art [43,60,61]. Solvent processing is presently the desired way to deposit thin-films, but does not provide a satisfying level of conductivity. Metallic phases are exceptional [23], because solvent processing can introduce residual extrinsic disorder (not least emerging from the low film thickness, impurity, solvent intercalation, abrupt interfaces). Vapor-processed polymers (VPPs) have shown higher degree of homogeneity and thus less extrinsic disorder finally leading to metallic CPs. VPPs are synthesized by chemical vapor deposition with the merit of united polymerization, doping and deposition [11,19,57,62–66]; however, here energetic disorder can arise through over-oxidation and the usage of aggressive oxidants in combination with heat. Ultimately, electropolymerization is an alternative successful, but elaborate method to obtain a metallic polymer [27,67,68].

2.3. Metal-insulator transition

At first glance, the quality of any conducting polymer becomes apparent by showing the conductivity (σ_r) inverse (or logarithmic) temperature profile (Fig. 3). In the insulating regime, the value of σ decreases by $T^{-\beta}$. The magnitude of the exponent β represents a measure of the proximity to the metallic state. In ideal case 0.25, it will be higher as extrinsic disorder is present (Eq. 1). The subsequent transition regime deviates from this power law with a gradually decreasing exponent. It should be narrow and approach the local conductivity minimum at the MIT. Thus, signatures of metallic conducting polymers are a low value of the relative resistivity (ρ_r), a narrow transition regime and β close to 0.25.

At sufficient low temperature, the minimum conductivity marks the actual metal-insulator transition. Until now, MITs have been reported in few polymer systems, among them PPy, PAni, PA and, recently, two types of PEDOT (acid-treated and VPP) and PBTTT (Fig. 4) [18,19,23,27,28,38].

The local conductivity minima (σ_{\min}) occur consistently between

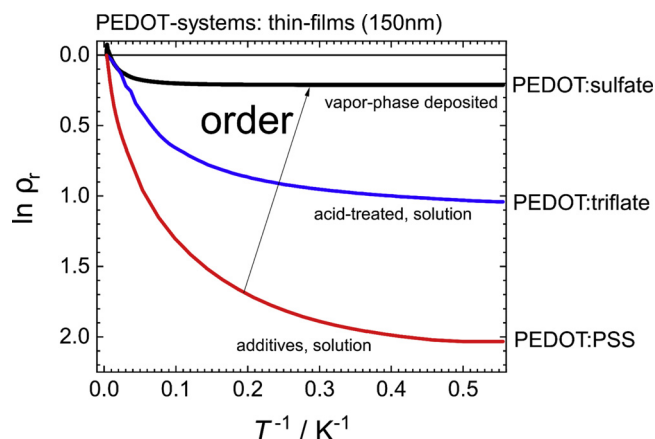


Fig. 3. Relative resistivity – inverse temperature profiles: Thin-films of PEDOT (with different processing techniques and different anions) show the effect of extrinsic disorder, in particular seen at low- T : (i) a higher ratio of the relative resistivity and (ii) stronger insulating and transition regime in case of higher disorder. Reproduced with permission from Ref. [18,59].

4–7 K at ambient pressure. Below these minima, the sign of TCR changes sign to positive (*i.e.* σ increases with decreasing temperature). These metallic polymers exemplify systems with practically no extrinsic disorder. Such situation is a direct result of careful processing and synthesis. The similar transition temperatures (4–7 K, Fig. 4) indicate that there exists a relation in conjugated systems: One hypothesis is that the intermolecular bonding strength is proportional to the transition energies $k_b T_{MIT}$. Assuming that intermolecular binding is characteristically van der Waals type, the final metal-insulator transition temperature will then depend on the radius among the polymer chains.

Thus, a reduction of the effective radius must rise the transition temperature T_{MIT} . Compressed metallic conducting polymers, polyacetylene (anisotropic), PPy and, recently, PEDOT (isotropic), show such temperature increase [19,26,69]. Based on these results, the relation of $k_b T_{MIT}$ and the interchain transfer integral have to be discussed in a greater picture [70,71].

2.4. Magnetoconductivity in the transition regime

Magnetoconductivity (MC) is useful study the metallic transition in conducting polymers. MC provides detailed insights to the scattering mechanism *i.e.* the magnitude of the average scattering length and, thus, the coherence among the molecules and the free charge carriers. This represents a valuable information, particularly to quantify the intensity of intermolecular overlap and the overall order.

In general, the magnetic field (B) induces carrier localization, *i.e.* it decreases the conductivity (magnetolocalization, ML). ML is observed in all CPs and relates to electron-electron interactions according to

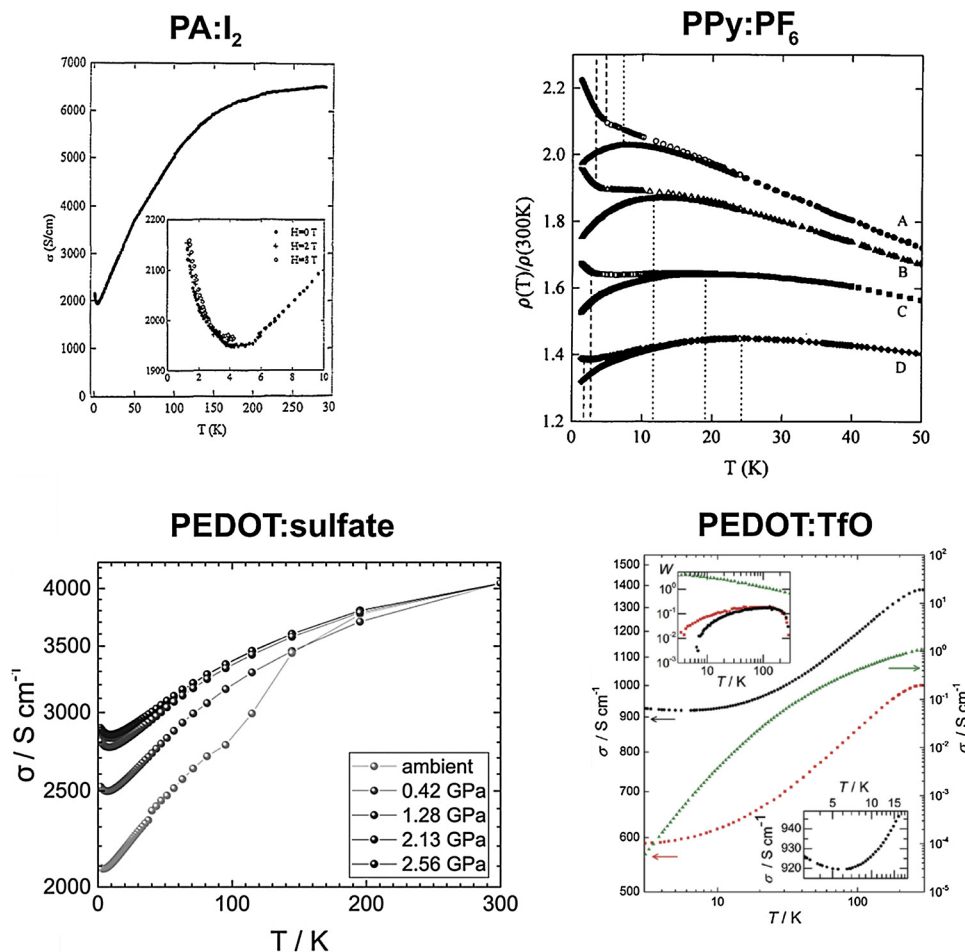


Fig. 4. Examples of metallic conducting polymers: Polyacetylene doped with iodine (PA:I₂, metal-insulator transition or conductivity minimum at 4 K), polypyrrole:PF₆ (PPy:PF₆, MIT at 7 K, other samples B, C, D are under pressure), poly-(3,4-ethylenedioxythiophene):sulfate (PEDOT:sulfate) and PEDOT:triflate, respectively, (MIT at 5 K and 6 K). Reproduced with permission from Ref. [19,23,27,28].

weak localization [19,28,76,42,43,46,55,72–75]. ML becomes stronger by decreasing temperature by the factor $T^{-3/2}$. The exact relation to B is a power law with quadratic exponent. In addition, every system has individual constants relating to the electron-electron interactions (discussed elsewhere) [72,73,77].

$$\Delta\sigma_{ML} = \sigma_{T,B} - \sigma_{T,B=0} = -const. \left(\frac{g\mu_B}{k_B}\right)^2 T^{-3/2} B^2 \quad (g\mu_B \cdot B < k_B T) \quad (2)$$

The final magnitude of ML depends on the ratio of $k_B T$ and B (derived by multiplication with μ_B (Bohr's magneton) and the g -factor, the gyromagnetic constant, ~ 2 for molecular matter). ML does not provide much information about extrinsic disorder.

In (semi)metallic CPs, however, there exists a second positive magnetic contribution to the conductivity (σ), which only depends on B and coherence: the positive magnetoconductivity (positive MC, $\Delta\sigma_{pos.MC}$). This effect is independent from the base conductivity ($\sigma_{B=0}$) of the system, and, therefore, can be considerably small as compared to the absolute value of σ and, particularly at low- T , as compared to the magnitude of ML. According to the Hikami-Larkin-Nagaoka equation, $\Delta\sigma_{pos.MC}$ relates to the quantum resonance of the field with a quadratic exponent in the orthogonal case (negligible spin-orbit coupling) [78]; its magnitude depends ultimately on the conductance quantum G_0 , the magnetic field and the coherence volume (volume element given by the mean-free-path of charge carriers, λ_{MFP}^3) (Eq. 3).

$$\Delta\sigma_{pos.MC} = +\left(\frac{1}{12\pi^2}\right) \left(\frac{e}{\hbar}\right)^2 G_0 \cdot \lambda_{MFP}^3 \cdot B^2 \quad (3)$$

In case of weak localization, ML and positive MC are additive effects: At low- T and low B , positive MC is dominant and gradually displaced by ML by increasing B . Subsequently one must zoom into the low- B regime in order to see the positive MC-effect at low temperatures (Fig. 5b and d). At higher temperatures, metallic CPs show only positive MC.

Positive MC is a characteristic phenomenon of weak localization and reported for conductors with intrinsic disorder such as doped silicon, metal alloys or amorphous metals. Thus, its occurrence in CPs shows a proximity to the metallic state, as it can only appear when charge carriers are sufficiently delocalized. Accordingly, positive MC can be used to derive the mean free path λ_{MFP} of the scattered charge carriers (Eq. 4), either by evaluating the magnitude of the slope (using σ vs. B^2 plot), or by taking the value of B at maximum magnetoconductivity indicating the optimum resonance condition between free charge carriers and magnetic field. For convenience, the latter can be plotted as the magnetic penetration depth or the Landau orbit size (L_D) to read out λ_{MFP} (Fig. 5e and Eq. 4).

$$\lambda_{MFP} \cong L_{D,max.MC} \quad \text{with} \quad L_D = \sqrt{\frac{\hbar}{e \cdot B}} \quad (4)$$

The magnitude of λ_{MFP} provides an estimation of the average electron coherence *i.e.* the order and strength of the intermolecular overlap. The advantage of the positive MC is that it occurs above the MIT, even in CPs without explicit MIT. It shows that there is substantial degree of delocalization and, overall, almost negligible amount of extrinsic disorder in the system.

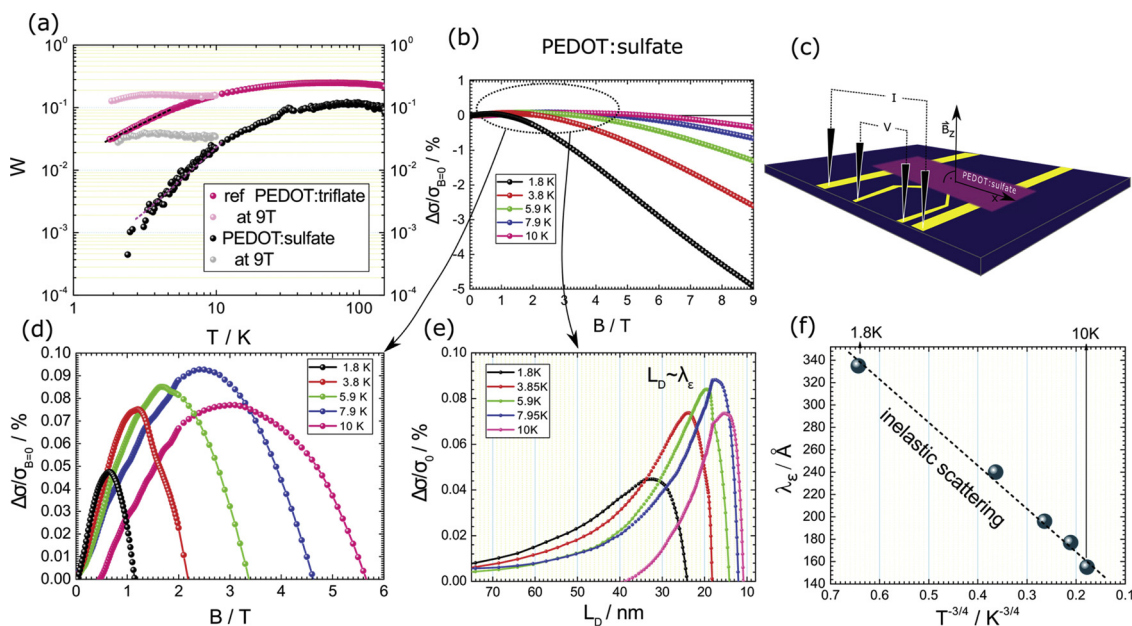


Fig. 5. Magnetoconductivity in metallic conducting polymer. (a) W (logarithmic derivative) of the conductivity *versus* $\log T$ shows the proximity to the metallic state, in particular for the black PEDOT:sulfate. The grey dots show the change of the conductivity at a magnetic field (B) of 9T (negative (*i.e.* decreasing) magnetoconductivity or magnetolocalization). (b) The same effect shown as absolute magnetoconductivity change (%): magnetolocalization particular stronger at low- T s and high B . (c) Schematic of the sample specimen: 4-wire probe. (d) Zoom in the positive part revealing a positive (*i.e.* increasing) magnetoconductivity *versus* B peaking at the maximum conductivity. The maximum shifts towards higher B as the temperature increases. (e) Plot of the positive magnetoconductivity using the magnetic penetration depth (the Landau orbit size, L_D) instead of B . The peak maximum corresponds to the mean free scattering path λ_{MFP} . (f) Fit of λ_{MFP} vs. $T^{-3/4}$ indicating the inelastic scattering (derived from weak localization) in the transition regime of the polymer. Reproduced with permission from Ref. [18].

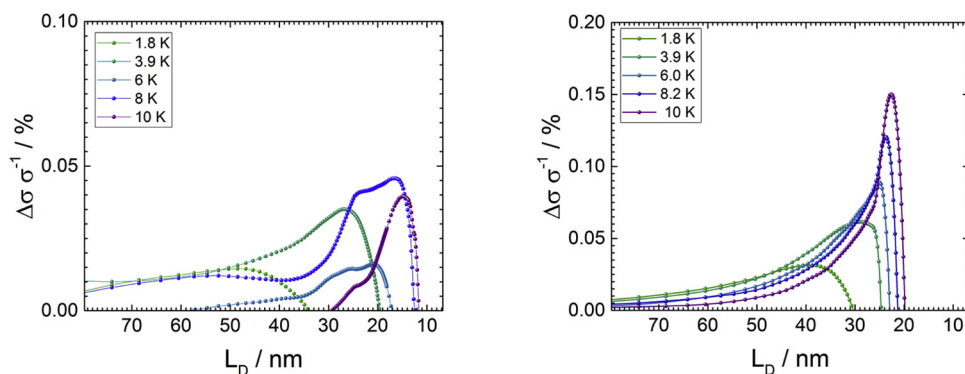


Fig. 6. Positive magnetoconductivity (relative magnetoconductivity *versus* the Landau orbit size L_D) at the metal-insulator transition. At ambient pressure (left) the positive magnetoconductivity shows a double-peak between 6 to 10 K, while under pressure (right) the entire system has a single-peak response and lower peak maxima. The latter case is interpreted as elastic scattering (transition temperature under pressure is 10 K), while the ambient sample is split in an elastic (low- T , 1.8 K and 3.9 K line) and both, ambivalent (double peak elastic and inelastic at 6 K, 8 K and 10 K). Reproduced with permission from Ref. [19].

λ_{MFP} scales with temperature by the exponential relation of $T^{-3/4}$ (weak localization) [47,59,76,79]. Such temperature-profile suggests inelastic scattering, however, only in the transition or insulating regime. At the conductivity minimum at the MIT, positive MC splits up into two peaks – one relating to inelastic, one to elastic scattering (Fig. 6).

Since inelastic scattering must be larger (damping term), such splitting could be an indication of a molecular phase transition. In the metallic regime, the positive MC merges to a single peak (Fig. 6). Here, the scattering is elastic. Such transition is in agreement with the sign-flip of the TCR and the rise of the conductivity. One conclusion is that the elastic-metallic regime relates to a molecular-structural phase transition, where the intermolecular overlap is substantially increased [69].

2.5. Mobility characterization

The Hall-effect in CPs has been frequently discussed [44,67,80–86]. Similar to the positive magnetoconductivity, the observation of the Hall-voltage indicates a band-structure and, thus, coherence among

molecules. In the metallic regime, the Hall-effect should be therefore similar as for metals, but up to now, there are no experimental data available. Fortunately, prior art has reported Hall measurements in the transition and insulating regime in various CPs [18,67,82,83].

One problem is there, that the transport is ambivalent and a fraction of the carriers is localized. Therefore, the Hall-voltage is substantially reduced by a disorder term connoted as Hall screening. Since its exact impact is difficult to quantify (because of temperature dependence), the evaluation of the Hall-voltage remains vague. Recently, a molecular phase model has been suggested that estimates the disorder parameters and the subsequent magnitude of Hall screening [44]. The model provides a solution in order to estimate the band mobility from the Hall-voltage in the insulating regime at or close to room temperatures. Empirically, however, such evaluation has to resolve the probing of tiny Hall-voltages and provide adequate fitting parameters to extract trustworthy band mobilities. Recently, lock-in measurements and careful model fits have reported reliable mobilities [82].

At low- T , in the transition regime close to the MIT, the Hall-voltage evaluation is less problematic. Since the phononic disorder is less intense, the magnitude is larger. Anyhow, disorder models are still

required in order to derive band mobilities [87,88]. The values for the band mobility are in the range of $30 \text{ cm}^2 \text{V}^{-1} \text{s}^{-1}$ [18]. The magnitude of the band mobility suggests that, ultimately, electrical transport in molecular systems remains mobility-limited. The results correlate to the coherence measured from magnetoconductivity.

Alternatively, or complementary to Hall, terahertz domain spectroscopy (THz) can be used to evaluate the band mobility and the DC conductivity [89–93]. The transmission spectra at low THz frequencies (e.g. around 0.13–3 THz) represent a non-destructive spectroscopic technique to study the DC conductivity and mobility. In (semi)metallic conducting polymers the classic Drude model can be used (assuming a single energy-independent scattering time) to model the spectra and obtain the (complex) conductivity and, by estimating the doping concentration n and effective mass m^* , the mobility (Eq. 5).

$$\hat{\sigma}(\omega) = \frac{ne^2\tau}{m^*(1 - i\omega\tau)} \quad (5)$$

For highly conducting polymers, THz parameters have been shown to be similar to electric measurements. However, for the case of rather low-conductivity systems, the classic Drude model is not appropriate. Such polymers require a more elaborate spectral fitting and aiding information (e.g. as proposed in the localized Drude model) [94]. Low-conductivity samples have been investigated using combined THz domain and infrared reflection spectroscopy to estimate the conductivity and mobility.

3. Conclusions and outlook

The emergence of a metal-insulator transition in conducting polymers, even when occurring at low temperatures, is an important step towards superior electrical transport. Isotropic metallic polymers can play a lead role as sustainable contenders for transparent conducting oxides, rare earth based magnets, noble metal catalysts and heavy metal thermoelectric active layers. The here discussed metallic phases in numerous polymers provides the evidence that extrinsic sources of disorder can be effectively suppressed with the consequence that low-temperature isotropic metallic phases are no longer exceptional. In particular combined processing and synthesis strategies represent successful routes to achieve superior homogeneity and isotropy – a clear advancement compared to earlier metallic polymers, which are dominated by nematic phases e.g. polyacetylene or to polypyrrole with explicit anisotropy factors.

Nonetheless, further efforts are required, particularly to improve the intrinsic properties. These are mainly the intense phonon scattering and the weakness of the intermolecular transfer integrals. Theoretical calculations as well as the here deeper discussed magnetotransport measurements show that both effects prevent metallic states at higher temperatures [95–97]. In order to increase the metallic character of polymers, one has to improve those intrinsic properties thus to shift the metal-insulator transition temperature towards room temperatures. This requires to strengthen the intermolecular binding [66,98]. Experimentally, this concept has been proven by using small ion doping, incorporation of stronger hydrogen binding among the molecules and by applying hydrostatic pressure. Consistently, these led to increase the metallic regime towards room temperature [27,49]. Such fully metallic polymers represent serious alternatives for the aforementioned applications in optoelectronics, magnetics and thermoelectrics, but also open new fields for instance (photo)electrocatalysis.

Acknowledgements

P.S. is grateful to the Austrian Exchange Service (OEAD,IN10/2015) for financial support. P.S. acknowledges the financial support from the Austrian Science Fund (FWF I3822-N37, “Sustainable Catalysis”). The author thanks N. Serdar Sariciftci and Reghu Menon for fruitful discussions. This project was supported by the European Regional

Development Fund (ERDF, IWB 2014-2020, 2018-98299, “Artificial Food”) and the your career grant from the Linz Institute of Technology (LIT, LIT-2017-4-YOU-005, “Conductive Biopolymer Carbonate Reduction”) at the Johannes Kepler University Linz.

References

- [1] O. Bubnova, Z.U. Khan, A. Malti, S. Braun, M. Fahlman, M. Berggren, X. Crispin, Optimization of the thermoelectric figure of merit in the conducting polymer poly(3,4-ethylenedioxythiophene), *Nat. Mater.* 10 (2011) 429–433, <https://doi.org/10.1038/nmat3012>.
- [2] Y.H. Kim, C. Sachse, M.L. Machala, C. May, L. Müller-Meskamp, K. Leo, Highly conductive PEDOT:PSS electrode with optimized solvent and thermal post-treatment for ITO-free organic solar cells, *Adv. Funct. Mater.* 21 (2011) 1076–1081, <https://doi.org/10.1002/adfm.201002290>.
- [3] N. Kim, B.H. Lee, D. Choi, G. Kim, H. Kim, J.-R. Kim, J. Lee, Y.H. Kahng, K. Lee, Role of Interchain Coupling in the metallic state of conducting polymers, *Phys. Rev. Lett.* 109 (2012) 106405, <https://doi.org/10.1103/PhysRevLett.109.106405>.
- [4] E. Jin Bae, Y. Hun Kang, K.-S. Jang, S. Yun Cho, Enhancement of thermoelectric properties of PEDOT: PSS and tellurium-PEDOT: PSS hybrid composites by simple chemical treatment, *Sci. Rep.* 6 (2016) 18805, <https://doi.org/10.1038/srep18805>.
- [5] J. Luo, D. Billep, T. Waechtler, T. Otto, M. Toader, O. Gordan, E. Sheremet, J. Martin, M. Hietschold, D.R.T. Zahn, T. Gessner, Enhancement of the thermoelectric properties of PEDOT:PSS thin films by post-treatment, *J. Mater. Chem. A Mater. Energy Sustain.* 1 (2013) 7576, <https://doi.org/10.1039/c3ta11209h>.
- [6] H. Park, S.H. Lee, F.S. Kim, H.H. Choi, I.W. Cheong, J.H. Kim, Enhanced thermoelectric properties of PEDOT:PSS nanofilms by a chemical dedoping process, *J. Mater. Chem. A Mater. Energy Sustain.* 2 (2014) 6532, <https://doi.org/10.1039/c3ta14960a>.
- [7] T. Park, C. Park, B. Kim, H. Shin, E. Kim, Flexible PEDOT electrodes with large thermoelectric power factors to generate electricity by the touch of fingertips, *Energy Environ. Sci.* 6 (2013) 788, <https://doi.org/10.1039/c3ee23729j>.
- [8] O. Bubnova, Z.U. Khan, A. Malti, S. Braun, M. Fahlman, M. Berggren, X. Crispin, Optimization of the thermoelectric figure of merit in the conducting polymer poly(3,4-ethylenedioxythiophene), *Nat. Mater.* 10 (2011) 429–433, <https://doi.org/10.1038/nmat3012>.
- [9] M. Scholdt, H. Do, J. Lang, A. Gall, A. Colmann, U. Lemmer, J.D. Koenig, M. Winkler, H. Boettner, Organic semiconductors for thermoelectric applications, *J. Korean Inst. Electr. Electron. Mater. Eng.* 39 (2010) 1589–1592, <https://doi.org/10.1007/s11664-010-1271-8>.
- [10] Y. Xia, K. Sun, J. Ouyang, Solution-processed metallic conducting polymer films as transparent electrode of optoelectronic devices, *Adv. Mater.* 24 (2012) 2436–2440, <https://doi.org/10.1002/adma.201104795>.
- [11] A. Ugur, F. Katmis, M. Li, L. Wu, Y. Zhu, K.K. Varanasi, K.K. Gleason, Low-dimensional conduction mechanisms in highly conductive and transparent conjugated polymers, *Adv. Mater.* 27 (2015) 4604–4610, <https://doi.org/10.1002/adma.201502340>.
- [12] B.J. Worfolk, S.C. Andrews, S. Park, J. Reinspach, N. Liu, M.F. Toney, S.C.B. Mannsfeld, Z. Bao, Ultrahigh electrical conductivity in solution-sheared polymeric transparent films, *Proc. Natl. Acad. Sci.* 112 (2015) 14138–14143, <https://doi.org/10.1073/pnas.1509581112>.
- [13] X. Crispin, F.L.E. Jakobsson, a Crispin, P.C.M. Grim, P. Andersson, a Volodin, C. van Haesendonck, M. Van der Auweraer, W.R. Salaneck, M. Berggren, 2006, 200, The origin of the high conductivity of (PEDOT–PSS) plastic Electrodes.pdf, *Chem. Mater.* 18 (2006) 4354–4360, <https://doi.org/10.1021/cm061032+>.
- [14] O. Bubnova, Z.U. Khan, H. Wang, S. Braun, D.R. Evans, M. Faretto, P. Hojati-Talemi, D. Dagnelund, J.-B. Arlin, Y.H. Geerts, S. Desbief, D.W. Breiby, J.W. Andreasen, R. Lazzaroni, W.M. Chen, I. Zozoulenko, M. Fahlman, P.J. Murphy, M. Berggren, X. Crispin, Semi-metallic polymers, *Nat. Mater.* 13 (2014) 190–194, <https://doi.org/10.1038/nmat3824>.
- [15] Aa. Farah, Sa. Rutledge, A. Schaarschmidt, R. Lai, J.P. Freedman, A.S. Helmy, Conductivity enhancement of poly(3,4-ethylenedioxythiophene)-poly(styrenesulfonate) films post-spincoating, *J. Appl. Phys.* 112 (2012) 113709, <https://doi.org/10.1063/1.4768265>.
- [16] A.J. Heeger, Semiconducting and metallic polymers: the fourth generation of polymeric materials, *J. Phys. Chem. B* 105 (2001) 8475–8491, <https://doi.org/10.1021/jp011611w>.
- [17] A.G. MacDiarmid, A.J. Heeger, Organic metals and semiconductors: the chemistry of polyacetylene, (CH)_x, and its derivatives, *Synth. Met.* 1 (1980) 101–118, [https://doi.org/10.1016/0379-6779\(80\)90002-8](https://doi.org/10.1016/0379-6779(80)90002-8).
- [18] D. Farka, H. Coskun, J. Gasiorowski, C. Cobet, K. Hingerl, L.M. Uiberlacker, S. Hild, T. Greunz, D. Stifter, N.S. Sariciftci, R. Menon, W. Schoefberger, C.C. Mardare, A.W. Hassel, C. Schwarzinger, M.C. Scharber, P. Stadler, Anderson-localization and the Mott-Ioffe-regel limit in glassy-metallic PEDOT, *Adv. Electron. Mater.* (2017) 1700050, <https://doi.org/10.1002/aeml.201700050>.
- [19] D. Farka, A.O.F. Jones, R. Menon, N.S. Sariciftci, P. Stadler, Metallic conductivity beyond the Mott minimum in PEDOT: sulphate at low temperatures, *Synth. Met.* 240 (2018) 59–66, <https://doi.org/10.1016/j.synthmet.2018.03.015>.
- [20] O. Bubnova, Z.U. Khan, H. Wang, S. Braun, D.R. Evans, M. Faretto, P. Hojati-Talemi, D. Dagnelund, J.-B. Arlin, Y.H. Geerts, S. Desbief, D.W. Breiby, J.W. Andreasen, R. Lazzaroni, W.M. Chen, I. Zozoulenko, M. Fahlman, P.J. Murphy, M. Berggren, X. Crispin, Semi-metallic polymers, *Nat. Mater.* 13 (2014) 190–194, <https://doi.org/10.1038/nmat3824>.
- [21] M.N. Gueye, A. Carella, N. Massonnet, E. Yvenou, S. Brenet, J. Faure-Vincent,

- S. Pouget, F. Rieutord, H. Okuno, A. Benayad, R. Demadrille, J.-P. Simonato, Structure and dopant engineering in PEDOT thin films: practical tools for a dramatic conductivity enhancement, *Chem. Mater.* 28 (2016) 3462–3468, <https://doi.org/10.1021/acs.chemmater.6b01035>.
- [22] T.-R. Chou, S.-H. Chen, Y.-T. Chiang, Y.-T. Lin, C.-Y. Chao, Highly conductive PEDOT:PSS films by post-treatment with dimethyl sulfoxide for ITO-free liquid crystal display, *J. Mater. Chem. C* 3 (2015) 3760–3766, <https://doi.org/10.1039/C5TC00276A>.
- [23] N. Massonnet, A. Carella, A. de Geyer, J. Faure-Vincent, J.-P. Simonato, Metallic behaviour of acid doped highly conductive polymers, *Chem. Sci.* 6 (2015) 412–417, <https://doi.org/10.1039/C4SC02463J>.
- [24] S. Kivelson, W.-P. Su, J.R. Schrieffer, A.J. Heeger, Missing bond-charge repulsion in the extended Hubbard model: effects in polyacetylene, *Phys. Rev. Lett.* 58 (1987) 1899–1902, <https://doi.org/10.1103/PhysRevLett.58.1899>.
- [25] M.J. Winokur, J. Maron, Y. Cao, A.J. Heeger, Disorder and staging in iodine-doped polyacetylene, *Phys. Rev. B* 45 (1992) 9656–9662, <https://doi.org/10.1103/PhysRevB.45.9656>.
- [26] Y. Cao, P. Smith, A.J. Heeger, Mechanical and electrical properties of highly oriented polyacetylene films, *Synth. Met.* 41 (1991) 181–184, [https://doi.org/10.1016/0379-6779\(91\)91033-7](https://doi.org/10.1016/0379-6779(91)91033-7).
- [27] R. Menon, C.O. Yoon, D. Moses, A.J. Heeger, Pressure and magnetic field dependence of the low temperature resistivity of PF6-doped polypyrrole, *Synth. Met.* 64 (1994) 53–57, [https://doi.org/10.1016/0379-6779\(94\)90274-7](https://doi.org/10.1016/0379-6779(94)90274-7).
- [28] R. Menon, Conductivity and magnetoconductance in iodine-doped polyacetylene, *Synth. Met.* 80 (1996) 223–229, [https://doi.org/10.1016/S0379-6779\(96\)03706-X](https://doi.org/10.1016/S0379-6779(96)03706-X).
- [29] C.O. Yoon, M. Reghu, A.J. Heeger, E.B. Park, Y.W. Park, K. Akagi, H. Shirakawa, Effect of anisotropy on conductivity and magnetoconductance in heavily doped polyacetylene, *Synth. Met.* 69 (1995) 79–80, [https://doi.org/10.1016/0379-6779\(94\)02372-6](https://doi.org/10.1016/0379-6779(94)02372-6).
- [30] K. Väkiparta, R. M. M.R. Andersson, Y. Cao, D. Moses, A.J. Heeger, Temperature dependence of the electrical conductivity of potassium-doped polyacetylene as a function of pressure and magnetic field, *Phys. Rev. B* 47 (1993) 9977–9980, <https://doi.org/10.1103/PhysRevB.47.9977>.
- [31] Y.-W. Park, A.J. Heeger, M.A. Dray, A.G. MacDiarmid, Electrical transport in doped polyacetylene, *J. Chem. Phys.* 73 (1980) 946–957, <https://doi.org/10.1063/1.440214>.
- [32] L.W. Shacklette, R.R. Chance, D.M. Ivory, G.G. Miller, R.H. Baughman, Electrical and optical properties of highly conducting charge-transfer complexes of poly(p-phenylene), *Synth. Met.* 1 (1980) 307–320, [https://doi.org/10.1016/0379-6779\(80\)90020-X](https://doi.org/10.1016/0379-6779(80)90020-X).
- [33] M. Nyman, O.J. Sandberg, S. Dahlström, D. Spoltore, C. Körner, Y. Zhang, S. Barlow, S.R. Marder, K. Leo, K. Vandeval, R. Österbacka, Doping-induced carrier profiles in organic semiconductors determined from capacitive extraction-current transients, *Sci. Rep.* 7 (2017) 5397, <https://doi.org/10.1038/s41598-017-05499-3>.
- [34] D. Brault, M. Lepinoy, P. Limelette, B. Schmaltz, F. Tran Van, Electrical transport crossovers and thermopower in doped polyaniline conducting polymer, *J. Appl. Phys.* 122 (2017) 225104, <https://doi.org/10.1063/1.5003576>.
- [35] R. Menon, C.O. Yoon, D. Moses, A.J. Heeger, Y. Cao, Transport in polyaniline near the critical regime of the metal-insulator transition, *Phys. Rev. B* 48 (1993) 17685–17694, <https://doi.org/10.1103/PhysRevB.48.17685>.
- [36] A.N. Aleshin, V.I. Kozub, D.-S. Suh, Y.W. Park, Low-temperature saturation of dephasing in heavily doped polyacetylene, *Phys. Rev. B* 64 (2001) 224208, <https://doi.org/10.1103/PhysRevB.64.224208>.
- [37] Y.W. Park, E.S. Choi, D.S. Suh, Metallic temperature dependence of resistivity in perchlorate doped polyacetylene, *Synth. Met.* 96 (1998) 81–86, [https://doi.org/10.1016/S0379-6779\(98\)00078-2](https://doi.org/10.1016/S0379-6779(98)00078-2).
- [38] T. Harada, H. Ito, Y. Ando, S. Watanabe, H. Tanaka, S. Kuroda, Signature of the insulator–metal transition of a semicrystalline conjugated polymer in ionic-liquid-gated transistors, *Appl. Phys. Express.* 8 (2015) 021601, <https://doi.org/10.7567/APEX.8.021601>.
- [39] S. Zanettini, J.F. Dayen, C. Etrillard, N. Leclerc, M.V. Kamalakar, B. Doudin, Magnetoconductance anisotropy of a polymer thin film at the onset of metallicity, *Appl. Phys. Lett.* 106 (2015) 063303, <https://doi.org/10.1063/1.4908526>.
- [40] A.I. Larkin, D.E. Khmel'nitskii, Activation conductivity in disordered systems with large localization length, *Sov. Phys. JETP* 56 (1982) 647–652.
- [41] H.T. Yi, Y.N. Gartstein, V. Podzorov, Charge carrier coherence and Hall effect in organic semiconductors, *Sci. Rep.* 6 (2016) 23650, <https://doi.org/10.1038/srep23650>.
- [42] K. Kang, S. Watanabe, K. Broch, A. Sepe, A. Brown, I. Nasrallah, M. Nikolka, Z. Fei, M. Heeney, D. Matsumoto, K. Marumoto, H. Tanaka, S. Kuroda, H. Siringhaus, 2D coherent charge transport in highly ordered conducting polymers doped by solid state diffusion, *Nat. Mater.* 15 (2016) 896–902, <https://doi.org/10.1038/nmat4634>.
- [43] P. Stadler, D. Farka, H. Coskun, E.D. Glowacki, C. Yumusak, L.M. Uiberlacker, S. Hild, L.N. Leonat, M.C. Scharber, P. Klapetek, R. Menon, N.S. Sariciftci, Local order drives the metallic state in PEDOT:PSS, *J. Mater. Chem. C* 4 (2016) 6982–6987, <https://doi.org/10.1039/C6TC02129H>.
- [44] H.T. Yi, Y.N. Gartstein, V. Podzorov, Charge carrier coherence and Hall effect in organic semiconductors, *Sci. Rep.* 6 (2016) 23650, <https://doi.org/10.1038/srep23650>.
- [45] S.D. Kang, G.J. Snyder, Charge-transport model for conducting polymers, *Nat. Mater.* 16 (2017) 252–257, <https://doi.org/10.1038/nmat4784>.
- [46] R.S. Kohlman, A. Zibold, D.B. Tanner, G.G. Ihas, T. Ishiguro, Y.G. Min, A.G. MacDiarmid, A.J. Epstein, Limits for metallic conductivity in conducting polymers, *Phys. Rev. Lett.* 78 (1997) 3915–3918, <https://doi.org/10.1103/PhysRevLett.78.3915>.
- [47] A.B. Kaiser, Electronic transport properties of conducting polymers and carbon nanotubes, *Rep. Prog. Phys.* 64 (2001) 1.
- [48] A. Aleshin, R. Kiebooms, R. Menon, A.J. Heeger, Electronic transport in doped poly(3,4-ethylenedioxythiophene) near the metal-insulator transition, *Synth. Met.* 90 (1997) 61–68, [https://doi.org/10.1016/S0379-6779\(97\)81227-1](https://doi.org/10.1016/S0379-6779(97)81227-1).
- [49] K. Lee, S. Cho, S. Heum Park, A.J. Heeger, C.-W. Lee, S.-H. Lee, Metallic transport in polyaniline, *Nature* 441 (2006) 65–68, <https://doi.org/10.1038/nature04705>.
- [50] A. Girlando, A. Painelli, Z.G. Soos, Electron/phonon coupling in conjugated polymers: Reference force field and transferable coupling constants for polyacetylene, *J. Chem. Phys.* 98 (1993) 7459–7465, <https://doi.org/10.1063/1.464684>.
- [51] K. Lee, A.J. Heeger, Optical investigation of intra and interchain charge dynamics in conducting polymers, *Synth. Met.* 128 (2002) 279–282, [https://doi.org/10.1016/S0379-6779\(02\)00006-1](https://doi.org/10.1016/S0379-6779(02)00006-1).
- [52] C. Cobet, J. Gasiorowski, D. Farka, P. Stadler, Polarons in conjugated polymers, in: K.-J. Hinrichs, Eichhorn Karsten (Eds.), *Ellipsom. Funct. Org. Surfaces Film*. 2018, pp. 355–387, https://doi.org/10.1007/978-3-319-75895-4_16.
- [53] C. Cobet, J. Gasiorowski, R. Menon, K. Hingerl, S. Schlager, M.S. White, H. Neugebauer, N.S. Sariciftci, P. Stadler, Influence of molecular designs on polaronic and vibrational transitions in a conjugated push-pull copolymer, *Sci. Rep.* 6 (2016) 35096, <https://doi.org/10.1038/srep35096>.
- [54] Y. Yamashita, T. Tsurumi, F. Hinkel, Y. Okada, J. Soeda, W. Zajęczkowski, M. Baumgarten, W. Pisula, H. Matsui, K. Müllen, J. Takeya, Transition between band and hopping transport in polymer field-effect transistors, *Adv. Mater.* 26 (2014) 8169–8173, <https://doi.org/10.1002/adma.201403767>.
- [55] R. Menon, C.O. Yoon, D. Moses, A.J. Heeger, Y. Cao, Transport in polyaniline near the critical regime of the metal-insulator transition, *Phys. Rev. B* 48 (1993) 17685–17694, <https://doi.org/10.1103/PhysRevB.48.17685>.
- [56] H. Wang, U. Ail, R. Gabrielsson, M. Berggren, X. Crispin, Ionic seebeck effect in conducting polymers, *Adv. Energy Mater.* 5 (2015) 1500044, <https://doi.org/10.1002/aenm.201500044>.
- [57] J.P. Lock, S.G. Im, K.K. Gleason, Oxidative chemical vapor deposition of electrically conducting poly(3,4-ethylenedioxythiophene) films, *Macromolecules* 39 (2006) 5326–5329, <https://doi.org/10.1021/ma060113o>.
- [58] K. Zuber, M. Fabretto, C. Hall, P. Murphy, Improved PEDOT conductivity via suppression of crystallite formation in Fe(III) tosylate during vapor phase polymerization, *Macromol. Rapid Commun.* 29 (2008) 1503–1508, <https://doi.org/10.1002/marc.200800325>.
- [59] D. Farka, H. Coskun, P. Bauer, D. Roth, B. Bruckner, P. Klapetek, N.S. Sariciftci, P. Stadler, Increase in electron scattering length in PEDOT:PSS by a triflic acid post-processing, *Monatsh. Chem. Chem. Mon.* 148 (2017) 871–877, <https://doi.org/10.1007/s00706-017-1973-1>.
- [60] Y. Honma, K. Itoh, H. Masunaga, A. Fujiwara, T. Nishizaki, S. Iguchi, T. Sasaki, Mesoscopic 2D charge transport in commonplace PEDOT:PSS films, *Adv. Electron. Mater.* 4 (2018) 1700490, <https://doi.org/10.1002/aeml.201700490>.
- [61] Y. Du, X. Cui, L. Li, H. Tian, W.-X. Yu, Z.-X. Zhou, Dielectric properties of DMSO-Doped-PEDOT:PSS at THz frequencies, *Phys. Status Solidi* 255 (2018) 1700547, <https://doi.org/10.1002/psb.201700547>.
- [62] P. Kovacic, G. del Hierro, W. Livernois, K.K. Gleason, Scale-up of oCVD: large-area conductive polymer thin films for next-generation electronics, *Mater. Horiz.* 2 (2015) 221–227, <https://doi.org/10.1039/C4MH00222A>.
- [63] X. Wang, A. Ugur, H. Goktas, N. Chen, M. Wang, N. Lachman, E. Kalfon-Cohen, W. Fang, B.L. Wardle, K.K. Gleason, Room temperature resistive volatile organic compound sensing materials based on a hybrid structure of vertically aligned carbon nanotubes and conformal oCVD/iCVD polymer coatings, *ACS Sens.* 1 (2016) 374–383, <https://doi.org/10.1021/acssensors.5b00208>.
- [64] A.M. Coclite, R.M. Howden, D.C. Borrelli, C.D. Petruczuk, R. Yang, J.L. Yagüe, A. Ugur, N. Chen, S. Lee, W.J. Jo, A. Liu, X. Wang, K.K. Gleason, 25th anniversary article: CVD polymers: a new paradigm for surface modification and device fabrication, *Adv. Mater.* 25 (2013) 5392–5423, <https://doi.org/10.1002/adma.201301878>.
- [65] S. Lee, K.K. Gleason, Enhanced optical property with tunable band gap of cross-linked PEDOT copolymers via oxidative chemical vapor deposition, *Adv. Funct. Mater.* 25 (2015) 85–93, <https://doi.org/10.1002/adfm.201402924>.
- [66] H. Coskun, A. Aljabour, P. De Luna, D. Farka, T. Greunz, D. Stifter, M. Kus, X. Zheng, M. Liu, A.W. Hassel, W. Schöfberger, E.H. Sargent, N.S. Sariciftci, P. Stadler, Biofunctionalized conductive polymers enable efficient CO₂ electro-reduction, *Sci. Adv.* 3 (2017) e1700686, <https://doi.org/10.1126/sciadv.1700686>.
- [67] T. Hasan Gilani, T. Masui, G.Yu. Logvenov, T. Ishiguro, Low-temperature Hall effect and thermoelectric power in metallic PF6-doped polypyrrole, *Synth. Met.* 78 (1996) 327–331, [https://doi.org/10.1016/0379-6779\(96\)80156-1](https://doi.org/10.1016/0379-6779(96)80156-1).
- [68] R. Menon, C.O. Yoon, D. Moses, Y. Cao, A.J. Heeger, Tuning through the critical regime of the metal-insulator transition in conducting polymers by pressure and magnetic field, *Synth. Met.* 69 (1995) 329–332, [https://doi.org/10.1016/0379-6779\(94\)02471-A](https://doi.org/10.1016/0379-6779(94)02471-A).
- [69] J. Ma, J.E. Fischer, Y. Cao, A.J. Heeger, X-ray structural study of trans-polyacetylene at high pressure, *Solid State Commun.* 83 (1992) 395–399, [https://doi.org/10.1016/0038-1098\(92\)90075-K](https://doi.org/10.1016/0038-1098(92)90075-K).
- [70] W.P. Su, J.R. Schrieffer, A.J. Heeger, Soliton excitations in polyacetylene, *Phys. Rev. B* 22 (1980) 2099–2111, <https://doi.org/10.1103/PhysRevB.22.2099>.
- [71] N.F. Mott, *Metal-Insulator Transitions*, Taylor & Francis LTD, 1974.
- [72] G. Bergmann, Physical interpretation of weak localization: a time-of-flight experiment with conduction electrons, *Phys. Rev. B* 28 (1983) 2914–2920, <https://doi.org/10.1103/PhysRevB.28.2914>.
- [73] G. Bergmann, Weak localization in thin films, *Phys. Rep.* 107 (1984) 1–58, [https://doi.org/10.1016/0370-1571\(84\)90001-1](https://doi.org/10.1016/0370-1571(84)90001-1).

- [doi.org/10.1016/0370-1573\(84\)90103-0](https://doi.org/10.1016/0370-1573(84)90103-0).
- [74] R. Menon, K. Väkiparta, Y. Cao, D. Moses, Pressure dependence of the conductivity and magnetoconductance in oriented iodine-doped polyacetylene, *Phys. Rev. B* 49 (1994) 16162–16170, <https://doi.org/10.1103/PhysRevB.49.16162>.
- [75] Y. Nogami, H. Kaneko, H. Ito, T. Ishiguro, T. Sasaki, N. Toyota, A. Takahashi, J. Tsukamoto, Low-temperature electrical conductivity of highly conducting polyacetylene in a magnetic field, *Phys. Rev. B* 43 (1991) 11829–11839, <https://doi.org/10.1103/PhysRevB.43.11829>.
- [76] P.W. Anderson, Absence of diffusion in certain random lattices, *Phys. Rev.* 109 (1958) 1492–1505, <https://doi.org/10.1103/PhysRev.109.1492>.
- [77] T.F. Rosenbaum, R.F. Milligan, G.A. Thomas, P.A. Lee, T.V. Ramakrishnan, R.N. Bhatt, K. DeConde, H. Hess, T. Perry, Low-temperature magnetoresistance of a disordered metal, *Phys. Rev. Lett.* 47 (1981) 1758–1761, <https://doi.org/10.1103/PhysRevLett.47.1758>.
- [78] S. Hikami, A.I. Larkin, Y. Nagaoka, Spin-orbit interaction and magnetoresistance in the two dimensional random system, *Prog. Theor. Phys. Suppl.* 63 (1980) 707–710, <https://doi.org/10.1143/PTP.63.707>.
- [79] I. Shlimak, M. Kaveh, State of Mott minimal metallic conductivity in a scaling approach to the metal-insulator transition in doped semiconductors, *Phys. Rev. B* 58 (1998) 15333–15335, <https://doi.org/10.1103/PhysRevB.58.15333>.
- [80] S. Wang, M. Ha, M. Manno, C. Daniel Frisbie, C. Leighton, Hopping transport and the Hall effect near the insulator–metal transition in electrochemically gated poly(3-hexylthiophene) transistors, *Nat. Commun.* 3 (2012) 1210, <https://doi.org/10.1038/ncomms2213>.
- [81] B. Lee, Y. Chen, D. Fu, H.T. Yi, K. Czelen, H. Najafov, V. Podzorov, Trap healing and ultralow-noise Hall effect at the surface of organic semiconductors, *Nat. Mater.* 12 (2013) 1125–1129, <https://doi.org/10.1038/nmat3781>.
- [82] P. Stadler, L.N. Leonat, R. Menon, H. Coskun, S. van Frank, C. Rankl, M.C. Scharber, Stable Hall voltages in presence of dynamic quasi-continuum bands in poly(3,4-ethylene-dioxythiophene), *Org. Electron.* 65 (2019) 412–418, <https://doi.org/10.1016/j.orgel.2018.12.001>.
- [83] K. Seeger, W.D. Gill, T.C. Clarke, G.B. Street, Conductivity and Hall effect measurements in doped polyacetylene, *Solid State Commun.* 28 (1978) 873–878, [https://doi.org/10.1016/0038-1098\(78\)90177-1](https://doi.org/10.1016/0038-1098(78)90177-1).
- [84] R.S. Klein, Investigation of the Hall effect in impurity-hopping conduction, *Phys. Rev. B* 31 (1985) 2014–2021, <https://doi.org/10.1103/PhysRevB.31.2014>.
- [85] T. Uemura, M. Yamagishi, J. Soeda, Y. Takatsuki, Y. Okada, Y. Nakazawa, J. Takeya, Temperature dependence of the Hall effect in pentacene field-effect transistors: possibility of charge decoherence induced by molecular fluctuations, *Phys. Rev. B* 85 (2012) 035313, <https://doi.org/10.1103/PhysRevB.85.035313>.
- [86] J.-F. Chang, T. Sakanoue, Y. Olivier, T. Uemura, M.-B. Dufourg-Madec, S.G. Yeates, J. Cornil, J. Takeya, A. Troisi, H. Sirringhaus, Hall-effect measurements probing the degree of charge-carrier delocalization in solution-processed crystalline molecular semiconductors, *Phys. Rev. Lett.* 107 (2011) 066601, <https://doi.org/10.1103/PhysRevLett.107.066601>.
- [87] L. Friedman, Hall conductivity of amorphous semiconductors in the random phase model, *J. Non. Solids* 6 (1971) 329–341, [https://doi.org/10.1016/0022-3093\(71\)90024-X](https://doi.org/10.1016/0022-3093(71)90024-X).
- [88] L. Friedman, N.F. Mott, The Hall effect near the metal-insulator transition, *J. Non. Solids* 7 (1972) 103–108, [https://doi.org/10.1016/0022-3093\(72\)90021-X](https://doi.org/10.1016/0022-3093(72)90021-X).
- [89] F. Yan, E.P.J. Parrott, B.S.-Y. Ung, E. Pickwell-MacPherson, Solvent doping of PEDOT/PSS: effect on terahertz optoelectronic properties and utilization in terahertz devices, *J. Phys. Chem. C* 119 (2015) 6813–6818, <https://doi.org/10.1021/acs.jpcc.5b00465>.
- [90] M. Yamashita, C. Otani, H. Okuzaki, M. Shimizu, Nondestructive measurement of carrier mobility in conductive polymer PEDOT:PSS using Terahertz and infrared spectroscopy, 2011 XXXth URSI Gen. Assem. Sci. Symp (2011) 1–4, <https://doi.org/10.1109/URSIGASS.2011.6050616>.
- [91] E. Nguema, V. Vigneras, J.L. Miane, P. Mounaix, Dielectric properties of conducting polyaniline films by THz time-domain spectroscopy, *Eur. Polym. J.* 44 (2008) 124–129, <https://doi.org/10.1016/j.eurpolymj.2007.10.020>.
- [92] T.-I. Jeon, D. Grischkowsky, A.K. Mukherjee, R. Menon, Electrical characterization of conducting polypyrrole by THz time-domain spectroscopy, *Appl. Phys. Lett.* 77 (2000) 2452–2454, <https://doi.org/10.1063/1.1319188>.
- [93] T.-I. Jeon, D. Grischkowsky, A.K. Mukherjee, R. Menon, Electrical and optical characterization of conducting poly-3-methylthiophene film by THz time-domain spectroscopy, *Appl. Phys. Lett.* 79 (2001) 4142–4144, <https://doi.org/10.1063/1.1427754>.
- [94] M. Yamashita, C. Otani, M. Shimizu, H. Okuzaki, Effect of solvent on carrier transport in poly(3,4-ethylenedioxythiophene)/poly(4-styrenesulfonate) studied by terahertz and infrared-ultraviolet spectroscopy, *Appl. Phys. Lett.* 99 (2011) 143307, <https://doi.org/10.1063/1.3647574>.
- [95] G. Brocks, Polarons and bipolarons in oligothiophenes: a first principles study, *Synth. Met.* 102 (1999) 914–915, [https://doi.org/10.1016/S0379-6779\(98\)00958-8](https://doi.org/10.1016/S0379-6779(98)00958-8).
- [96] P. Vogl, D.K. Campbell, First-principles calculations of the three-dimensional structure and intrinsic defects in trans-polyacetylene, *Phys. Rev. B* 41 (1990) 12797–12817, <https://doi.org/10.1103/PhysRevB.41.12797>.
- [97] U. Salzner, Electronic structure of conducting organic polymers: insights from time-dependent density functional theory, *Wiley Interdiscip. Rev. Comput. Mol. Sci.* 4 (2014) 601–622, <https://doi.org/10.1002/wcms.1194>.
- [98] H. Coskun, A. Aljabour, L. Uiberlacker, M. Strobel, S. Hild, C. Cobet, D. Farka, P. Stadler, N.S. Sariciftci, Chemical vapor deposition - based synthesis of conductive polydopamine thin-films, *Thin Solid Films* 645 (2018) 320–325, <https://doi.org/10.1016/j.tsf.2017.10.063>.